Polymer 50 (2009) 4520–4528

Contents lists available at ScienceDirect

Polymer

journal homepage: www.elsevier.com/locate/polymer

Synthesis and characterization of soluble copoly(arylene ether sulfone phenyl-s-triazine)s containing phthalazinone moieties in the main chain

Guipeng Yu [a,c], Cheng Liu [a,b,c], Hongxin Zhou [a,c], Jinyan Wang [a,b,c], Encheng Lin [a,c], Xigao Jian [a,c,*]

[a] State Key Laboratory of Fine Chemicals, Dalian University of Technology, Dalian 116012, Liaoning, China
[b] Liaoning High Performance Resin Engineering Research Center, Dalian 116012, China
[c] Department of Polymer Science and Materials, Dalian University of Technology, Dalian 116012, China

ARTICLE INFO

Article history:
Received 7 April 2009
Received in revised form
8 July 2009
Accepted 13 July 2009
Available online 24 July 2009

Keywords:
Poly(arylene ether)s
Phenyl-s-triazine
Phthalazinone

ABSTRACT

A series of new poly(arylene ether sulfone phenyl-s-triazine) copolymers containing phthalazinone moieties in the main chain (PPESPs) were prepared by a direct solution polycondensation of 4-(4-hydroxylphenyl)(2*H*)-phthalazin-1-one (HPPZ) with 2-phenyl-4,6-bi(4-fluorophenyl)-1,3,5-triazine (BFPT) and 4,4′-dichlorodiphenyl sulfone (DCS). Model reactions monitored by HPLC indicated that BFPT had slightly higher reactivity than DCS in nucleophilic displacement reactions. The obtained random copolymers were characterized by FTIR, NMR, elemental analysis and GPC. The presence of sulfone and phthalazinone in the polymer chain results in an improvement in the solubility of poly(arylene ether phenyl-s-triazine)s in common organic solvents, such as *N*-methylpyrrolidone, *N*,*N*-dimethyl acetamide (DMAc), chloroform, sulfolane and pyridine. Thermal analysis reveal that the copolymers exhibit high glass transition temperatures (T_gs) ranging from 271–300 °C, and excellent thermal stability associated with decomposition temperatures for 5% mass-loss exceeding 503 °C. All copolymers are amorphous except PPESP28 as evidenced by WAXD. Their T_gs and solubility increase with an increase in sulfone content in the polymer backbone, while the crystallinity and overall thermal stability appear to decrease. This kind of phthalazinone-based copoly(arylene ether sulfone phenyl-s-triazine)s may be considered a good candidate for using as high-performance structural materials.

1. Introduction

Processable and heat-temperature polymeric materials have received extensive interest, due to the constant requirement for high-performance polymers as viable replacements for materials such as ceramics and metals in the automotive, aerospace and microelectronic industries [1]. Aromatic s-triazine-based polymers, among the most thermally stable polymers reported, have recently gained a lot of interest academically and industrially mainly due to their unique structure features [2–4]. The incorporation of s-triazine units into aromatic polymer chain enhances the rigidity of their backbone, and also leads to strong charge transfer interactions between s-triazine rings and aromatic rings. Therefore, this kind of polymers always possesses an attracting balance of excellent thermal stability, good chemical resistance, high tensile strengths and modulus even at elevated temperatures [5–7].

As a kind of newly developed heterocycle-containing polymers, poly(arylene ether phenyl-s-triazine)s (PAEPs) are particularly valuable in high-temperature applications as thin films for electroluminescent devices or matrix resins for advanced composites [8–11]. For example, PAEPs derived from 4,4′-hexafluorobisphenol A have been used as hole blocking/electron transport layers for application in multilayer light-emitting diodes (LEDs), since the high electron affinity and structural symmetry of the s-triazine units favor electron injection and transport [9,10]. In general, PAEPs are a class of amorphous or micro-crystalline polymers with glass transition temperatures (T_gs) exceeding 240 °C as well as acceptable mechanical properties and excellent thermooxidative stability. Although very few PAEPs have been reported in the literature, either low-molecular-weight oligomers or intractable resins were frequently obtained, because the strong charge transfer interactions among the aromatic or heterocyclic rings make the PAEPs insoluble in most organic solvents. For example, high-viscosity PAEPs derived from hydroquinone, 4,4′-biphenol or 2,7-naphthalenediol exhibit high glass transition temperatures and excellent thermooxidative stability associated with high decomposition temperatures ($T_{5\%}$ in excess of 550 °C in air) [8], but they are insoluble in most organic solvents except hot DMAc. Primarily because of the polymers' insolubility, it is

* Corresponding author. State Key Laboratory of Fine Chemicals, Dalian University of Technology, Dalian 116012, Liaoning, China. Tel.: +86 411 83653426; fax: +86 411 83639223.
E-mail address: jian4616@dl.cn (X. Jian).

0032-3861/$ – see front matter © 2009 Elsevier Ltd. All rights reserved.
doi:10.1016/j.polymer.2009.07.030

rather difficult to process this type of thermally stable polymers. Their films or membranes can be hardly obtained except by using melt compression molding at extremely high temperatures. In addition, the synthetic reaction conditions for these PAEPs are a little rigorous due to the insolubility of the polymers in the reaction media. High-molecular-weight PAEPs are generally prepared in diphenylsulfone at the temperatures exceeding 190 °C. The limited solubility and rigorous synthetic reaction conditions hamper the syntheses, characterization, processing and widespread application of PAEPs, especially of high-molecular-weight materials. These problems have initiated a search for soluble PAEPs by using structural modification of chain in recent years, with a view to simplifying synthesis, improving processability and hence broadening their applications, especially adhesives, coatings and membranes. The incorporation of flexible linkages [12], pendent groups [13], kink, non-coplanar units [14], or non-linear moieties [15] into the thermally stable polymer backbones, has been employed to achieve good solubility in typical organic solvents while maintaining the other unique properties. Our group has demonstrated the syntheses of a number of polymers, including poly(arylene ether)s [16], polyamides [17], polyimides [18] as well as other types of polymers [19], whose solubility has been favorably improved by the introduction of phthalazinone moieties into the polymer backbone. Such polymers were disclosed with acceptable thermal stabilities as well as reasonable solubility in selected aprotic polar solvents, like *N*,*N*-dimethyl acetylamide and *N*-methylpyrrolidone. Therefore, the phthalazinone has been proved to be a high efficiency unit for improving solubility of thermally stable polymers.

In continuation of our efforts to develop processable and heat-resistant polymers, we here attempted to prepare a series of new highly oragnosoluble PAEP polymers by incorporating phthalazinone and sulfone moieties into their rigid chain. In this article, we disclosed the synthesis, characterization and properties of copoly(arylene ether sulfone phenyl-s-triazine)s containing phthalazinone moieties in the main chain (simplified as PPESPs). Copolymers with different contents of sulfone and phenyl-s-triazine were derived from 4-(4-hydroxylphenyl)(2*H*)-phthalazine-1-one (HPPZ) with 2-phenyl-4,6-bi(4-fluorophenyl)-1,3,5-triazine (BFPT) and 4,4′-dichlorodiphenyl sulfone (DCS) by the one-step solution polycondensation under mild reaction conditions. The syntheses of these copolymers together with the reactivity of the dihalogenated monomers in nucleophilic displacement reactions were discussed. The effects of the introduction of phthalazinone and sulfone moieties on the solubility, crystallinity and thermal properties of the copolymers were also examined.

2. Experimental

2.1. Materials

2-Phenyl-4,6-bi(4-fluorophenyl)-1,3,5-triazine (BFPT) was synthesized according to the procedure reported previously [9]. The product was obtained as white long thin needles; m.p.: 260.2–260.8 °C; the product was confirmed by MALDI-TOF/MS. GC/MS (M+ Calcd. as $C_{21}H_{13}N_2F_2$ 345.1078): $m/z = 345.1067$ (M+).

4-(4-Hydroxylphenyl)(2*H*)-phthalazin-1-one (HPPZ) was prepared as white powder by the method reported in Ref. [20]. The product was obtained as white powder; m.p.: 310.0–310.8 °C; yield: 90 wt%; the product was confirmed by MALDI-TOF/MS. GC/MS (M+ Calcd. as $C_{14}H_{10}O_2N_2$ 238.0742): $m/z = 238.0750$ (M+).

4,4′-Dichlorodiphenyl sulfone (DCS) was purified by recrystallization from isopropanol and dried in a vacuum oven for 24 h. Anhydrous potassium carbonate (Beijing Chemical Co., A.R.) was ground and dried in vacuum at 100 °C for 24 h before use. Sulfolane (Beijing Chemical Co., A.R.) was dried and vacuum distilled over sodium hydroxide pellets (Beijing Chemical Co., A.R.), then the middle fractions were collected and stored over molecular sieves (type 4 Å) before use. Toluene was distilled over calcium hydride under reduced pressure. Unless otherwise specified, all other solvents and reagents were purchased from Beijing Chemical Co. and used as received.

2.2. Instruments

Inherent viscosities (η_{inh}) of the copolymers were measured by Ubbelohde capillary viscometer at a concentration of 0.5 g/dL in *N*-methylpyrrolidone (NMP) or concentrated sulfuric acid at 25 °C according to their solubility. Infrared measurements were performed on a Thermo Nicolet Nexus 470 Fourier transform infrared (FTIR) spectrometer. ^{1}H NMR (400 MHz), ^{1}H ^{1}H gCOSY NMR (400 MHz) and ^{13}C NMR (100 MHz) spectra were obtained with a Varian Unity Inova 400 spectrometer at an operating temperature of 25 °C using $CDCl_3$ as a solvent and the data were listed in parts per million downfield from tetramethylsilane (TMS). ^{19}F NMR (376 MHz) spectra were obtained under the same conditions as for ^{1}H NMR and the data were listed in parts per million downfield from potassium fluoride (KF). High performance liquid chromatogram (HPLC) was performed on a Hewlett–Packard (HP) 1100 liquid chromatograph using a mixture of acetic acid (0.1 wt%) and methanol (v/v = 90:10) as eluting solvent and a 2.0 × 150 mm Microbore column (Waters Spherisorb® S5 ODS2) as column. Gel permeation chromatography (GPC) analysis was carried out on a HP 1090 HPLC instrument equipped with 5 μm Phenogel columns (linear, 4 × 500 Å) arranged in series with chloroform as solvent and a UV detector at 254 nm. And the values were calibrated versus polystyrene standard. Matrix-assisted laser desorption ionization time-of-flight mass spectroscopy (MALDI-TOF-MS) analyses were performed on a Micromass GC-TOF CA 156 MALDI-TOF/MS. Elemental analysis was measured on a Vario ELIII CHNOS Elementaranalysator from Elementaranalysesyteme GmbH. Thermogravimetric analysis (TGA) and derivative thermogravimetric analysis (DTG) of the copolymer were performed on a Mettler TGA/SDTA851 thermogravimetric analysis instrument in a nitrogen atmosphere at a heating rate of 20 °C min^{-1} from 100 to 800 °C. Decomposition temperature (T_d) was taken as the temperature of 5% and 10% weight loss. Temperature for the maximum weight loss rate (T_{max}) in nitrogen was also measured at a heating rate of 20 °C min^{-1}. Char yield (C_y) was calculated as the percentage of solid residue after heating from 100 to 800 °C in flowing nitrogen. The glass transition temperature (T_g) was determined with a Mettler DSC822 differential scanning calorimetry (DSC) in flowing nitrogen at a heating rate of 10 °C min^{-1} from 50 to 400 °C. Wide-angle X-ray diffraction (WAXD) was performed at room temperature on a Rigaku D/max 2400 automatic X-ray diffractometer with Ni-filtered Cu Kα radiation (40 V, 100 mA).

2.3. Model reaction

The model reactions of BFPT and DCS with excess phenol were carried in similar procedures, and the model compounds produced were labeled as BFPT-P and DCS-P, respectively. A typical synthetic procedure of BFPT-P was given as an example. A 250 mL three-necked round-bottomed flask, equipped with a mechanical stirrer, nitrogen gas inlet tube and a Dean-Stark trap was charged with phenol (21.6 mmol), K_2CO_3 (excess, 25.9 mmol) and rinsed with 10 mL sulfolane and 20 mL toluene. The mixture was stirred and heated to the reflux temperature (140–150 °C) for 4 h to effect dehydration of the system. After the produced water was azeotroped off with toluene, the reaction mixture was cooled to room temperature. BFPT (9.0 mmol) was charged into the flask and then

the reaction mixture was heated stepwise to 190 °C. The reaction mixture was maintained at this temperature for 6 h, following the progress of the displacement reaction by high performance liquid chromatogram (HPLC). The resultant reaction solution was poured into hot distilled water (500 mL) with stirring and the precipitated products were then rinsed with hot distilled water to remove inorganic salts. The crude products were further purified by an overnight extraction using a Soxhlet extractor with acetone and then dried at 120 °C under vacuum for 24 h. Selected data of BFPT-P: Yield: 99 wt%. M.p.: 140.3–141.5 °C (according to DSC scan). FT-IR (KBr, cm^{-1}): 3066 (Ar–H), 1608, 1586, 1521 (C=N or C=C), 1488, 1417, 1369, 1241 (C–O), 1146, 829, 779. ^{1}H NMR (400 MHz, $CDCl_3$, ppm) δ: 8.65–8.85 (d, 6H), 7.50–7.64 (m, 3H), 7.31–7.45 (m, 4H), 6.97–7.31 (m, 10H). TOF/MS. GC/MS (M+ Calcd. as $C_{33}H_{23}N_3O_2$, 493.1790) *m/z*: 493.1784 (M+). Elem. Anal. Calcd. for $C_{33}H_{23}N_3O_2$: C, 80.31; H, 4.70; N, 8.51%. Found: C, 80.58; H, 5.05; N, 8.54%. Selected data of DCS-P: Yield: 98 wt%. M.p.: 144.5–146.3 °C (according to DSC scan). FT-IR (KBr, cm^{-1}): 3066 (Ar–H), 1582 (C=N or C=C), 1487, 1411, 1321 (SO_2, symmetric), 1245 (C–O), 1149, 1107 (SO_2, asymmetric), 840, 766. ^{1}H NMR (400 MHz, $CDCl_3$, ppm) δ: 7.82–7.86 (d, 4H), 7.32–7.40 (m, 4H), 7.17–7.25 (m, 2H), 6.96–7.04 (m, 8H). TOF/MS. GC/MS (M+ Calcd. as $C_{24}H_{18}SO_4$, 402.0926) *m/z*: 402.0917 (M+). Elem. Anal. Calcd. for $C_{24}H_{18}SO_4$: C, 71.63; H, 4.51; S, 7.97%. Found: C, 71.39; H, 5.17; S, 8.04%.

2.4. Synthesis of PPESP copolymers

The PPESP copolymers were synthesized via a nucleophilic aromatic substitution (S_NAr), as depicted in Scheme 1. The numbers of the sample name indicated the molar fractions of DCS and BFPT. For example, the resultant copolymer in the copolymerization starting from 60 mol percents of DCS and 40 mol percents of BFPT could be labeled as PPESP64. All copolymers were prepared in a similar procedure as for the model reactions described above. Therefore, only the synthesis of PPESP64 was described briefly below. A mixture of HPPZ (5.0 mmol), K_2CO_3 (6.0 mmol), 2 mL sulfolane and 25 mL toluene was stirred and refluxed for 3 h at 150 °C under the protection of nitrogen, and then toluene and the produced water were distilled off completely. Subsequently, DCS (3.0 mmol), BFPT (2.0 mmol) and 1 mL sulfolane was added into the flask at room temperature, and the mixture was maintained under stirring at 190 °C for 6 h. The resultant viscous reaction mixture was slowly poured into hot distilled water (200 mL) with vigorous stirring, and the precipitated copolymer was then rinsed six times with hot distilled water. The dried product was further purified by dissolving in NMP and then being filtered through a thin layer of celite. Then the filtrate was slowly poured into ethanol with stirring, and the resulting suspension was filtered. Finally, the purified product was dried at 120 °C under vacuum for 24 h. The yield of PPESP64 was 93 wt%. Selected data of PPESP64: IR (KBr, cm^{-1}): 3064 (=C–H), 1669 (C=O), 1587, 1502 (C=C or C=N), 1445, 1364 (C–N), 1304 (SO_2, symmetric), 1237 (C–O), 1152 (SO_2, asymmetric), 846, 685 (C–S–C). ^{1}H NMR (400 MHz, $CDCl_3$, ppm) δ: 8.71–8.82 (m, 12H), 8.55 (s, 5H), 8.01–8.03 (d, 12H), 7.92–7.99 (m, 15H), 7.71–7.74 (d, 4H), 7.64–7.66 (d, 10H), 7.46–7.48 (d, 4H), 7.20–7.22 (d, 8H), 7.19–7.20 (d, 10H), 7.11–7.16 (d, 12H), 7.10–7.13 (d, 10H). ^{13}C NMR (100 MHz, $CDCl_3$, ppm) δ: 171.45, 170.75, 161.3, 160.54, 158.78, 157.48, 156.23 147.93, 147.52, 146.98, 145.80, 145.63, 145.32, 140.19, 139.63, 136.05, 135.69, 134.96, 133.71,133.43, 132.16, 131.42, 131.14, 129.34, 128.61, 128.17, 126.82, 126.98, 125.43, 120.15, 119.50, 118.59, 118.41. Elem. Anal. Calcd. for PPESP64 $(C_{148}H_{90}O_{16}N_{16}S_3)_n$ $(2442.59)_n$: C, 73.50; H, 3.60; N, 8.91%. Found: C, 71.27; H, 3.81; N, 8.89%.

3. Results and discussion

3.1. Model reaction

The reactions utilized for the synthesis of BFPT-P and DCS-P were the nucleophilic aromatic substitutions on a halide at the *para* positions on the phenyl groups which were attached to s-triazine and sulfone group, respectively. As shown in Scheme 1, the model reaction of 20% excess phenol with activated dihalogenated monomer, DCS or BFPT, was accomplished by using anhydrous potassium carbonate as a base. The excess base here was used to covert the phenol into the more reactive phenolates. Since potassium carbonate is a weak base, no hydrolytic side reaction with BFPT or DCS was observed. The model reactions were performed in sulfolane in the presence of a minimal amount of toluene to allow azeotropic distillation of the water formed as a byproduct in the reactions. The expected products, BFPT-P and DCS-P, were isolated as single homogeneous products in essentially quantitative yields (exceeding 98%). The results obtained from FTIR, NMR, GC-TOF and elemental analysis are in good accordance with the chemical structure of the target products (see Section 2.3). Apart from the desired product DCS-P, no side products formed, which demonstrates that the chloride substituents *para* to the sulfone group are cleanly displaced by phenolates. DCS, which is activated by the electron-withdrawing sulfone substituent, can accept the negative charge developed through the formation of a Meisenheimer complex and hence become more susceptible towards nucleophilic aromatic substitution reaction [21]. In case of BFPT, the fluoride

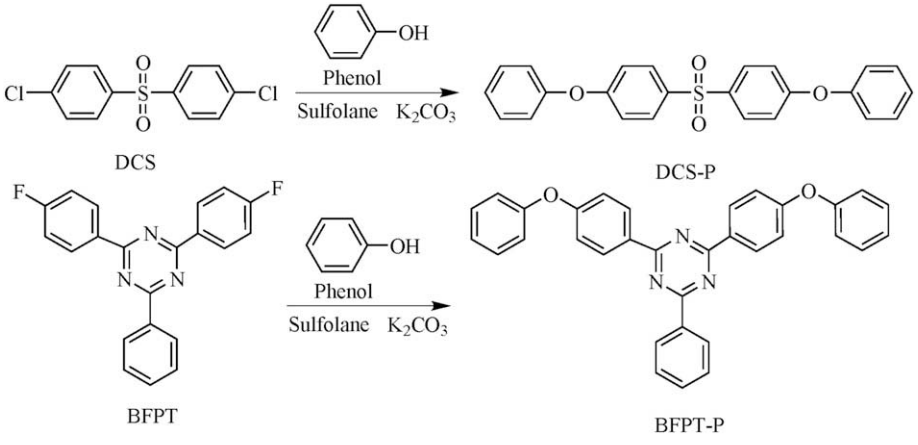

Scheme 1. Model reactions of BFPT and DCS with phenol.

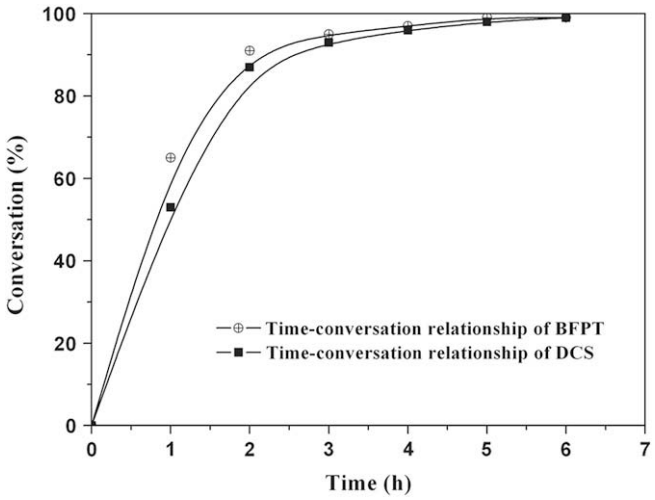

Fig. 1. The time–conversation relationships of BFPT and DCS in model reactions.

substituents in the *para*-orientation of the s-triazine nuclei were cleanly displaced by phenolates in the model reaction as evidenced by ^{19}F NMR, ^{1}H NMR and HPLC instruments. High selectivity and good yield observed in this model reaction demonstrate this transformation is very suitable as polymer-forming reactions. The good reactivity of BFPT in nucleophilic halo displacement is mainly attributed to the following two factors. First, a Meisenheimer complex would easily form a stabilized intermediate during the transformation due to resonance of the negative charge into the s-triazine nuclei, analogous to conventional activating groups (e.g., sulfone, ketone) [21,22]. Second, facile nucleophilic aromatic substitution of *o*-aryl halides from an s-triazine-substituted benzene ring should occur since the heterocycle is a typical strong electron-withdrawing group. The electronic effect of the s-triazine ring on the 2-phenyl group was evaluated by ^{1}H NMR, as the deshielding of the protons *ortho* to a substituent is indicative of an electron-withdrawing group. A comparison of the ^{1}H NMR data of BFPT, 4,4′-difluorodiphenyl sulfone and 4,4′-difluorobenzophenone shows the deshielding of the aromatic protons *ortho* to the s-triazine heterocycle ($\delta = 8.8$) verse the aromatic protons *ortho* to a ketone group ($\delta = 7.9$) and a sulfone group ($\delta = 8.0$), more conventional activating groups, to be greater with respect to electron affinity. To demonstrate the relative reactivity of BFPT and DCS in nucleophilic substitution, their model reactions were conducted under the same reaction conditions and the changes of their concentrations were monitored by HPLC at an interval of 1 h, respectively. Shown in Fig. 1 are the calculated conversions of BFPT and DCS which are observed to increase from an original point as a function of the reaction time. It is clearly seen that the fluoride of BFPT demonstrates slightly higher reactivity than the chloride of DCS in nucleophilic substitution reactions, which could be attributed to the strong electron-withdrawing effect of the s-triazine rings *para* to leaving groups, plus the easy detachability of fluorine atoms.

3.2. Polymer synthesis

Model reaction has demonstrated that BFPT has high activity towards nucleophilic displacement reaction and hence can act as a novel starting material for the preparation of PAEPs. The PPESP copolymers with different compositions were synthesized via the solution polycondensation of HPPZ with various ratios of DCS and BFPT under similar conditions as for the model reactions, as shown in Scheme 2. For comparison, poly(phthalazinone ether sulfone) (simplified as PPES) and poly(phthalazinone ether phenyl-s-triazine) (simplified as PPEP) homopolymers were also prepared in the similar procedures. Although the incorporation of phthalazinone groups into the backbone tends to be effective in improving the overall solubility of the PAEPs to some extent, high-viscosity polymers (exceeding 0.60 dL/g) could hardly be obtained under the described conditions since they may crystallize and precipitate before the formation of high-molecular-weight polymers. Therefore, both the solubility and viscosity are not sufficiently high to fabricate uniform and flexible films by spin coating or other solution casting techniques. The intrinsic viscosity (η_{inh}) of the PPES synthesized is 1.21 dL/g, and it significantly increases and reaches a maximum (2.25 dL/g) when the polycondensation time was prolonged to 14 h. The number-average molecular weight (M_n) of PPES, which was measured in chloroform by GPC, increases from 25,400 to 45,200 (Table 1). This may occur because of the much better solubility of PPES in sulfolane compared with that of PPEP. In these copolymerizations, sulfolane or dipolar aprotic solvents such as NMP, *N*,*N*-dimethyl acetamide (DMAc), were experimentally suitable solvents, because they effectively dissolve the monomers, the polar intermediates and the high-molecular-weight polymers formed. Although NMP or DMAc tends to be good solvents and is easier to handle, sulfolane was used in these copolymerization reactions since allowing higher reaction temperatures (e.g., 190 °C, etc) which is required to maintain solubility of the copolymers.

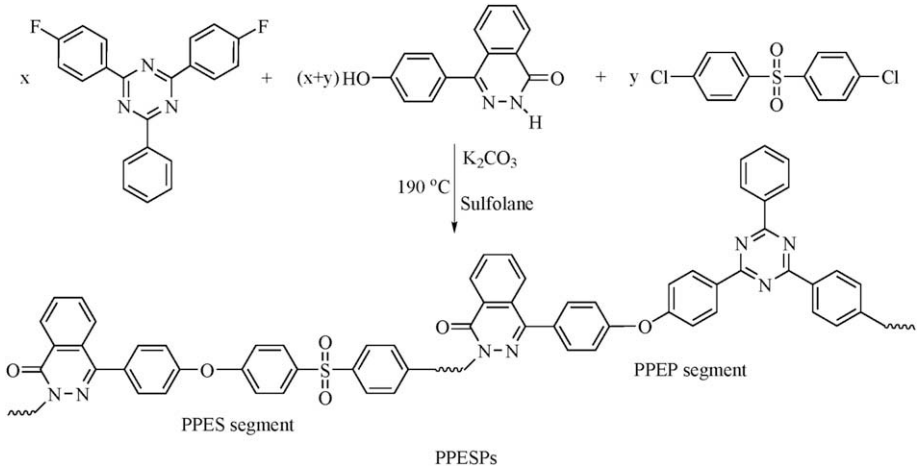

Scheme 2. The synthetic route of PPESPs.

Table 1
Synthetic data and physical properties of PPEP, PPES and PPESPs.

Polymer	Composition DCS/BFPT	Reaction time (h)	η_{inh}[a] (dL/g)	M_n[b]	PD[b]	Yield (%)	Color
PPEP	0/100	4.0	0.57[c]	–[d]	–[d]	98	White
PPESP28	20/80	4.5	0.80	–[d]	–[d]	93	White
PPESP46	40/60	5.5	0.62	16,700	3.2	93	White
PPESP55	50/50	5.5	0.76	18,900	3.5	93	White
PPESP64	60/40	6.0	1.18	22,500	2.5	92	White
PPESP82	80/20	6.0	0.91	19,800	3.4	93	White
PPES	100/0	6.0	1.21	25,400	3.1	94	White
PPES	100/0	14.0	2.25	45,200	3.5	95	White

[a] Determined at a concentration of 0.5 g/dL in NMP at 25 °C.
[b] Determined number-average molecular weight and polydispersities by GPC calibrated with polystyrene standards.
[c] Determined at a concentration of 0.5 g/dL in concentrated sulfuric acid at 25 °C.
[d] Not detected.

Additionally, sulfolane has been shown to be an excellent solvent for PPESs' syntheses [23]. All copolymerization reactions proceeded homogeneously and smoothly in common organic solvents, thus the synthetic conditions for these copolymers are much milder than those for the known PAEPs.

DCS and BFPT were added into the reaction system at one time, reacting with DHPZ by a competition of their reaction activity. As indicated in Table 1, the higher the feed ratio is of BFPT to DCS, the shorter the polycondensation time is that is needed for a high intrinsic viscosity. This may occur because of the slightly higher reactivity of BFPT compared with that of DCS which is in good agreement with the dihalides' relative reactivity discussed above. However, the difference of the dihalide reactivity was very minor as evidenced by the model reactions, suggesting that every activated dihalide almost has a similar opportunity to react with HPPZ throughout the copolymerization. Therefore, it was impossible for any dihalide monomer to form a relatively long block chain according to the statistical theory and almost random copolymers would be obtained. By this means, the extent of block copolymerization can be controlled to a desirable extent, as evidenced by the improved organic solubility and NMR analysis of the PPESP copolymers.

Among the copolymers investigated, the lower η_{inh} and M_n values are exhibited by PPESP28 and PPESP46, but their η_{inh} values are still much larger than that of PPEP homopolymer (Table 1). These results indicate that the PPES segments are helpful to improve the solubility of the copolymers in polar organic solvents and form truly high-molecular-weight copolymers. Interestingly, a consistent increase in the M_n or η_{inh} values is not observed as the sulfone content increases in the copolymer backbone. Both the M_n and η_{inh} reach maximum when the molar sulfone content was 60 percent relative to the total dihalides. These phenomenons could be easily explained, considering the above-discussed crystallization effect of PPEP segments and the slightly higher reactivity of BFPT relative to that of DCS as concluded in Section 3.1. All the PPESP copolymers and homopolymers (PPEP and PPES) were obtained as white fibrous materials in 92–98% yields.

3.3. Polymer characterization

The key structural features of the copolymers synthesized were characterized using instrumental techniques including FTIR, NMR and elemental analysis. As shown in Fig. 2, disappearance of absorptions in the range of 3200–3500 cm^{-1} indicates the complete conversion of O–H and N–H groups. Characteristic stretching bands of sulfone groups appearing at 1304 cm^{-1} (SO_2, symmetric), 1152 cm^{-1} (SO_2, asymmetric) and 685 cm^{-1} (C–S–C), whose intensity increases with the increase of sulfone content, indicate that different content of sulfone group has been introduced into the polymer chain successfully during the reaction. The presence of phenyl-s-triazine is identified by the strong absorption bands at 1587, 1502 cm^{-1} (C═N stretch) and 1364 cm^{-1} (C–N stretch). The absorption bands of lactam C═O in phthalazinone appear at around 1670 cm^{-1} and the bands for Ph–O–Ph linkages at around 1240 cm^{-1}, which correlate sufficiently well with the expected structure of the copolymers.

As a representative example, H–H gcosy NMR spectrum of PPESP55 and the chemical shift assignment of relative hydrogen protons are illustrated in Fig. 3. A comparison of ^{1}H NMR spectra of several representative copolymers, PPESP46, PPESP64 and PPESP82, are shown in Fig. 4. The characteristic peaks shifting downfield at 8.55 ppm, which can always be used as the reference signal to assign the other atoms, is diagnostic for the presence of *ortho*-hydrogen (H-1) of lactam in phthalazinone. The presence of phenyl-s-triazine in the main chain of copolymers is identified by signals at 8.71–8.82, 7.71–7.74, 7.46–7.48 and 7.20–7.22 ppm. The hydrogen protons (H-8, H-9, H-12) *ortho* to s-triazine nuclei appear at high frequencies (8.71–8.82) due to the deshielding ring current effect of the strong electron-withdrawing s-triazine nuclei. The four signals at 8.01–8.03 ppm are ascribed to the aromatic hydrogen protons (H-15, H-16) *ortho* to sulfone group. In addition, the integration intensity of characteristic peaks of H-15 and H-16 increases while that of H-8, H-9 and H-12 reduces with an increase in the content of sulfone. As shown in Figs. 3 and 4, ^{1}H NMR spectrum of PPESP82 is well distinguished in the region of 7.8–8.2 ppm, whereas the protons in PPESP64, PPESP55 and PPESP46 cannot be

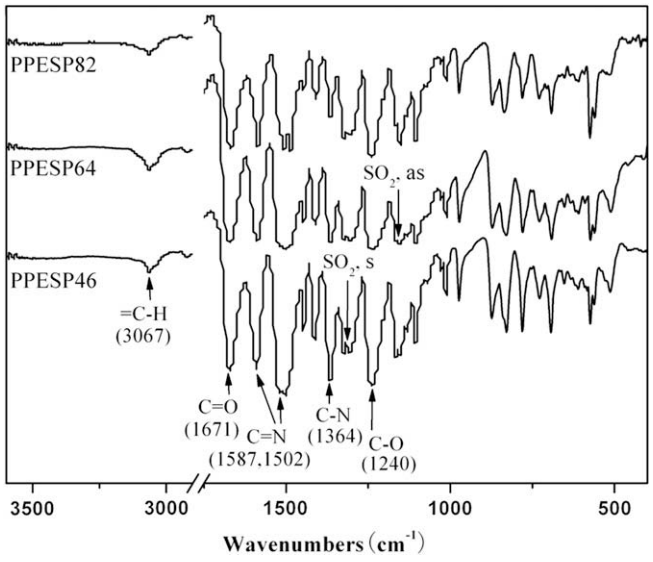

Fig. 2. FTIR spectra of PPESP82, PPESP64 and PPESP46.

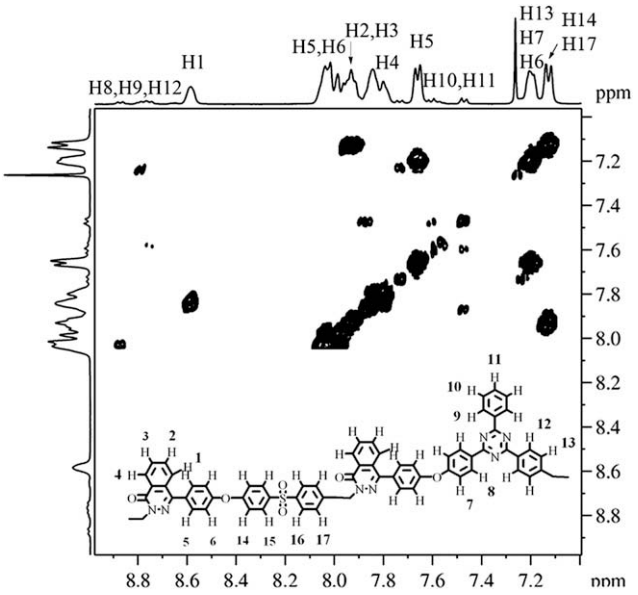

Fig. 3. H–H gcosy NMR spectrum of PPESP55 in $CDCl_3$.

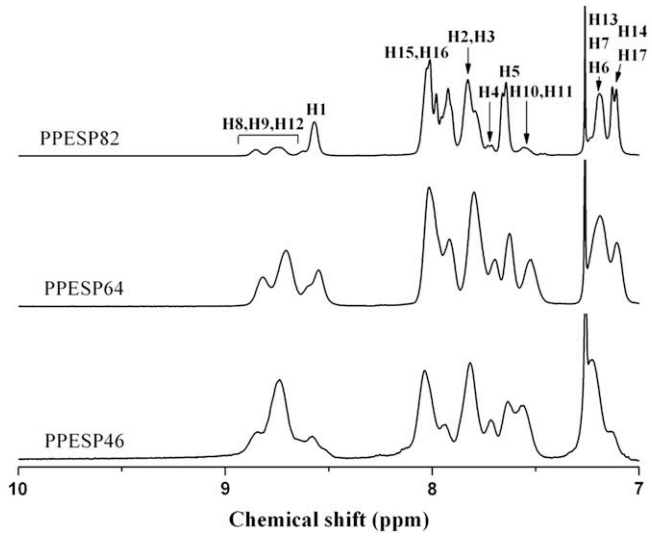

Fig. 4. ^1H NMR spectra of PPESP82, PPESP64 and PPESP46 in $CDCl_3$.

separated clearly in the same region, suggesting that the sequences in the latter copolymers are somewhat "short block" or "random". ^{13}C NMR spectra of the obtained copolymers in $CDCl_3$ were also found to be in well accordance with their chemical structure. For example, in a representative ^{13}C NMR spectrum of PPESP64, the signals for the carbon protons of the lactam carbonyl groups in phthalazinone appear at 158.59 ppm (see Section 2.4). The presence of phenyl-s-triazine groups is also identified by signals at 171.45 and 170.75 ppm which are assigned to the carbon protons of the s-triazine nuclei. The carbon signals of the s-triazine nuclei appear at high frequencies due to its deshielding ring current effect. The tested values by the element analysis of the synthesized copolymers are in reasonable agreement with the calculated values (Table 2), which also provide helpful evidence for identifying the chemical structure of copolymers.

3.4. Polymer solubility

The solubility behavior of the resulting copolymers was studied in various organic solvents by dissolving 0.04 g of the polymers in 1 mL solvent (4%, w/v) at different temperatures. As summarized in Table 3, at ambient temperatures most copolymers are highly soluble in several aprotic polar solvents, such as DMAc, NMP and even in less polar solvents like Py, consistent with the reports on PPES homopolymers [23]. The copolymers can also resolve in sulfolane, *N*,*N*-dimethyl foramide (DMF) and dimethylsulfoxide (DMSO) at elevated temperatures. In addition, they exhibit good solubility in the chlorinated solvents including chloroform and in less efficient solvent dichloromethane except PPESP28 and PPESP46. All copolymers can be easily cast into transparent flexible films through their solutions using NMP or DMAc as solvent. For this reason, these new PPESP copolymers could possibly be used in applications other than those of the known PAEPs and conventional poly(arylene ether)s, such as membrane and coating applications. In summary, the copolymers exhibit much better solubility compared with Victrex® PEEK and the known PAEPs. The improved solubility may be resulted from the introduction of the crank, twisted non-coplanar phthalazinone and the kinked sulfone moieties into the main chain which cumbers the close packing of the intermolecular chains and enlarges the average intermolecular distance of polymers, thus enabling solvent molecules to diffuse easily into the polymer chains. Additionally, copolymerization in this study seems to aid the creation of random irregularities along the polymer backbone, and might also contribute to the polymer–solvent intermolecular interactions and hence good solubility. Most of the copolymers except PPESP82 can hardly resolve in THF, isopropanol, acetone, benzene, toluene and chlorobenzene, even at elevated temperatures (Table 3). The overall solubility of the copolymers decreases as the content of phenyl-s-triazine increases in the polymer chain. This may be attributed to the strengthening charge transfer interactions between phenyl-s-triazine rings and aromatic rings which hamper solvent molecules to diffuse into the copolymer chains.

3.5. Thermal properties

Differential scanning calorimetry (DSC), thermogravimetric analyses (TGA) and derivative thermogravimetric analysis (DTG) measurements were applied to study the thermal behavior of the resulting copolymers in nitrogen atmosphere and the results are summarized in Table 4. DSC, TGA and DTG thermograms of the synthesized copolymers are illustrated in Figs. 5–7, respectively. As could be expected from the molecular structure, the copolymers exhibit transitions in the region of high temperatures exceeding 271 °C (taking as the midpoint of the change in slope of the baseline in DSC curve), indicating their good heat resistance, and no clear evidence of crystallinity was observed by the DSC measurements in any case. It is apparent that the DSC heating scans reveal only single distinct T_g for each copolymer and the T_g values increase gradually with the sulfone content, which approximately fits the rule of

Table 2
Composition and elemental data of PPEP, PPES and PPESPs.

Polymer	Formula	Elemental analysis					
		Calc.			Found		
		C	H	N	C	H	N
PPEP	$(C_{35}H_{21}N_5O_2)_n$	77.34	3.89	12.88	78.18	3.91	12.79
PPESP28	$(C_{166}H_{100}O_{12}N_{22}S_3)_n$	74.81	3.96	12.09	76.22	3.85	11.89
PPESP46	$(C_{157}H_{95}O_{14}N_{19}S_2)_n$	74.37	3.77	10.50	73.05	3.92	10.47
PPESP55	$(C_{61}H_{37}O_6N_7S)_n$	73.56	3.72	9.71	73.94	3.61	9.67
PPESP64	$(C_{148}H_{90}O_{16}N_{16}S_3)_n$	73.50	3.60	8.91	71.27	3.81	8.89
PPESP82	$(C_{139}H_{85}O_{18}N_{13}S_4)_n$	71.95	3.42	7.24	72.61	3.43	7.29
PPES	$(C_{26}H_{16}O_4N_2S)_n$	69.01	3.56	6.19	70.33	3.59	6.21

Table 3
Solubility of PPEP, PPES and PPESPs.

Polymer[a]	Solubility[b]												
	NMP	Dc[c]	Sf	DM	Py	DMF	CF	CCl	CB	IP	To	Bz	THF
PPEP	++	++	+	+	+	−	−	−	−	−	−	−	−
PPESP28	++	+−	+	+	+	−	−	−	−	−	−	−	−
PPESP46	++	++	+	+	+	+	++	−	−	−	−	−	−
PPESP55	++	++	+	+	++	++	++	+	−	−	−	−	−
PPESP64	++	++	+	+	++	++	++	+	−	−	−	−	−
PPESP82	++	++	+	+	++	++	++	++	−	−	−	−	−
PPES	++	++	+	+	++	++	++	++	−	−	−	−	−
PAEP[d]	−	+	−	−	−	−	−	−	−	−	−	−	−
PEEK[e]	−	−	−	−	−	−	−	−	−	−	−	−	−

[a] Tested with 0.04 g of the polymers in 1 mL of solvent.
[b] Solubility: ++: soluble in room temperature; +: soluble on heating; +−: partially soluble on heating; −: insoluble.
[c] NMP: *N*-methylpyrrolidone; Dc: *N*,*N*-dimethyl acetamide; Sf: sulfolane; DM: dimethylsulfoxide; Py: pyridine; CF: chloroform; CCl: dichloromethane; CB: chlorobenzene; IP: isopropanol; To: toluene; Bz: benzene; THF: tetrahydrofuran.
[d] PAEP was prepared by the reaction of 4,4′-biphenol and BFPT according to Ref. [8].
[e] Victrex® PEEK.

random copolymers (Fig. 5). The introduction of the polar sulfone groups into the backbone leads to an increase in intermolecular chain interactions that hampers the movement of the polymer chains, as shown by T_g. In addition, the free volume of the copolymers may decrease as the decreasing content of bulky phenyl-s-triazine units, leading to a decrease in T_g value.

According to Fox equation [24], the T_gs of random copolymers could be predicted based on the feed ratio of the dihalides as presented in Fig. 8 (solid line) using the following equation:

$$\frac{1}{T_g} = \frac{W_1}{T_{g1}} + \frac{W_2}{T_{g2}} \quad (1)$$

where T_g is the glass transition temperature of the copolymer, W_1 is the weight fraction of BFPT relative to the total dihalide, W_2 is the weight fraction of DCS relative to the total dihalide, T_{g1} and T_{g2} are the glass transition temperatures of the PPEP ($T_{g1} = 269\ ^\circ C$) and PPES ($T_{g2} = 305\ ^\circ C$) [23], respectively. A good agreement of the T_g values of the copolymers with values predicted by Fox equation according to the feed ratios was also observed (Fig. 8). Therefore, the T_gs of the PPESPs investigated can be tailored by varying the molar sulfone content in main chain. As shown in Table 4, the T_gs of the copolymers and PPEP are higher than those of the known PAEPs ($T_g = 240$–$255\ ^\circ C$) [8,9] and Victrex® PEKK ($T_g = 144\ ^\circ C$) [25]. These results demonstrate that the incorporation of rigid phthalazinone is an effective way to raise T_gs and improve the heat resistance of PAEPs.

As shown in Fig. 6 and Table 4, all copolymers exhibited high thermal stability with no significant weight loss up to temperatures of approximately 450 °C in nitrogen. The temperatures for 5% and 10% mass-loss of the copolymers are higher than 503 °C and 515 °C under nitrogen, respectively. In addition, these two values decrease gradually with the increase in sulfone content except those of PPESP46. In case of PPESP46, these values are slightly lower than those of the PPESP55 and PPESP64. This is possibly due to the higher concentration of chain ends of PPESP46 relative to the others, as implied by the low inherent viscosity and M_n. Among the investigated copolymers, highest $T_{5\%}$ and $T_{10\%}$ values are exhibited by PPESP28, due to the highest content of the phenyl-s-triazine units that endows the copolymer with the highest resonance energy along the chain. The thermal stability of these copolymers is only a little lower than that of PPEP analogue and the known PAEPs, and much higher than that of the PPES homopolymers, as evidenced by thermogravimetric data listed in Table 4. Therefore, good thermal stability of the copolymers is maintained relative to PPEP with the introduction of the sulfone moieties into the backbone. The copolymers show char yields (C_y) of 53–63%, when heated to 800 °C under a nitrogen atmosphere, confirming their excellent thermal stability. The C_y value increases gradually with increase of the content of the phenyl-s-triazine unit in the copolymer chains, most probably due to the phenyl-s-triazine that has higher char concentration than sulfone at the elevated temperatures.

Table 4
Thermal properties of PPEP, PPES and PPESPs.

Polymer	T_g[a] (°C)	T_g[b] (°C)	$T_{5\%}$[c] (°C)	$T_{10\%}$[c] (°C)	$T_{20\%}$[c] (°C)	T_{max}[d] (°C)	C_y[e] (%)
PPEP	269	–	536	563	627	536, 617[f]	67
PPESP28	271	275	519	534	590	529, 620[f]	63
PPESP46	279	282	508	517	549	526, 619[f]	60
PPESP55	283	285	515	526	548	526, 617[f]	56
PPESP64	289	289	513	524	539	527	55
PPESP82	300	297	503	515	533	529	53
PPES	305	–	505	512	533	527	53
PAEP[g]	241	–	604	610	–	606	53
PEEK[h]	143	–	569	–	–	587	–

[a] Glass transition temperature tested by DSC at a heating rate of 10 °C/min in nitrogen.
[b] Calculated from Fox Equation (Formula (1)).
[c] Temperature for 5%, 10% and 20% weight loss in nitrogen, heating rate of 20 °C/min.
[d] Temperature for the maximum in nitrogen, heating rate of 20 °C/min.
[e] Char yield calculated as the percentage of solid residue after heating from 100 to 800 °C in nitrogen.
[f] Two peaks in the DTG curves.
[g] PAEP was prepared by the reaction of 4,4′-biphenol and BFPT according to Ref. [8].
[h] Victrex® PEEK, data according to Ref. [25].

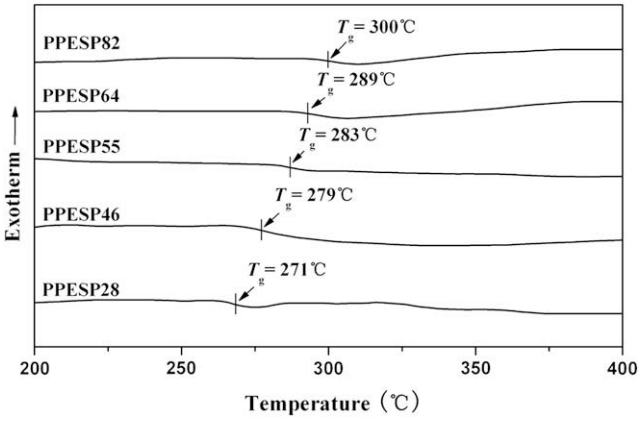

Fig. 5. DSC traces of PPESPs.

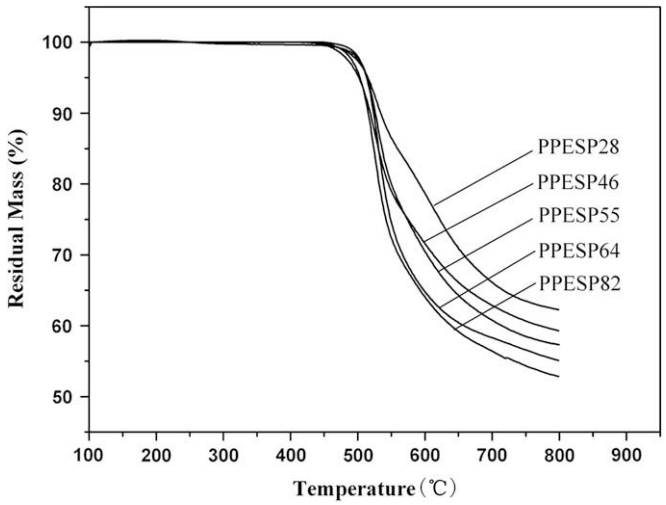

Fig. 6. TGA thermograms of PPESPs.

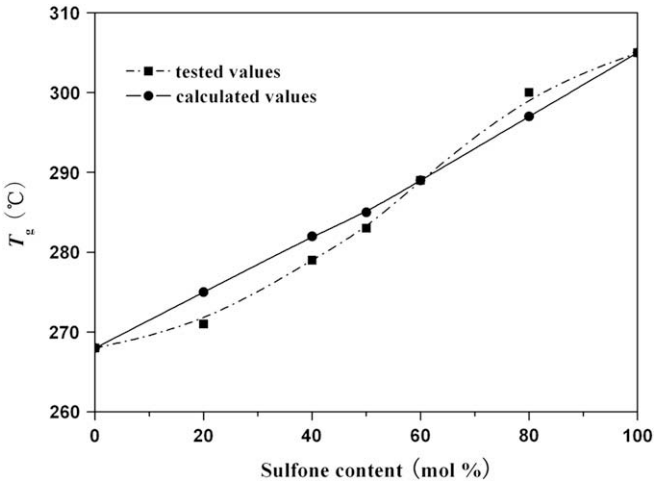

Fig. 8. Correlation between T_g value of PPESPs and the sulfone content (mol% relative to the total dihalides). (■) The dash dot line represents the experimental values determined from DSC. (●) The solid line represents the calculated values according to Fox equation.

It is clearly observed that there are two decomposition stages at temperatures higher than 520 °C in the DTG curves of PPESP28, PPESP46 and PPESP55 (Fig. 7), similar to those of the PPEP analogues. The first and second degradation stages occur at near 526 °C and 619 °C, respectively. Interestingly, DTG study on PPES indicates that there is single degradation stage occurring at near 527 °C, almost at the same temperature of the copolymers' first stage. In cases of PPESP64 and PPESP82, the second degradation stages in the region of higher temperatures also exist but are not as clear as the others, indicating that the thermal decompositions of these sulfone-rich copolymers are accelerated relative to those of phenyl-s-triazine-rich copolymers. Since the phenyl-s-triazine unit endows its polymers with high resonance energy along the chain and it also has relatively high activation energy for thermal decomposition [2], it would be reasonable that this unit is considered as the most thermally stable moiety in the polymer chain. Therefore, the first degradation stage starting at around 526 °C could possibly be resulted from the degradation of the sulfone groups or rearrangement of phthalazinone groups in the copolymer backbone [26,27].

Based on the results as listed in Table 4, it can be concluded that all these synthesized copolymers exhibit high T_g, $T_{5\%}$, $T_{10\%}$ and C_y values, thus being extremely thermally stable. The overall thermal stability increases with the decreasing content of sulfone in the main chain. The high thermal stability of PPESP copolymers will make them as potential high-temperature polymeric materials in a wide range of applications (e.g., high-temperature fuel cells, advanced composites, etc). Further efforts in these aspects are currently underway by our group.

3.6. Polymer crystallinity

Crystallinity of the copolymers synthesized was investigated by means of wide-angle X-ray diffraction (WAXD) on powder samples at room temperature. Fig. 9 illustrates the WAXD patterns of two typical copolymers, PPESP28 and PPESP64. The calculated crystallinity degree of the copolymers is almost negligible except that of PPESP28, and therefore, they are amorphous. Interestingly, four weak diffraction peaks are displayed in the WAXD pattern of PPESP28, giving a pattern typical of micro-crystalline nature. In addition, the intensity of these diffraction peaks reduces gradually

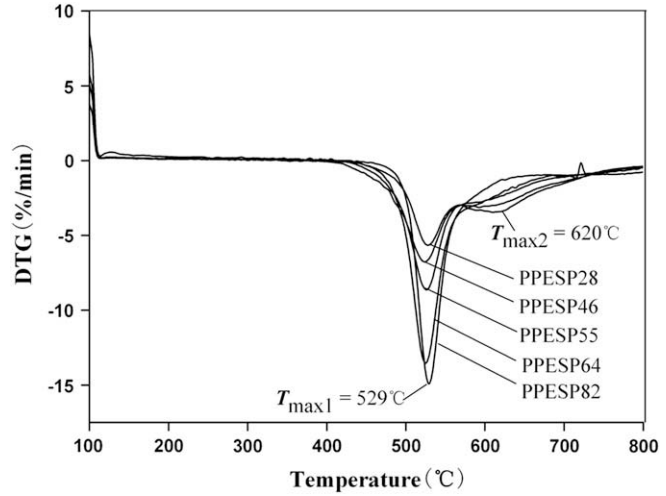

Fig. 7. DTG thermograms of PPESPs.

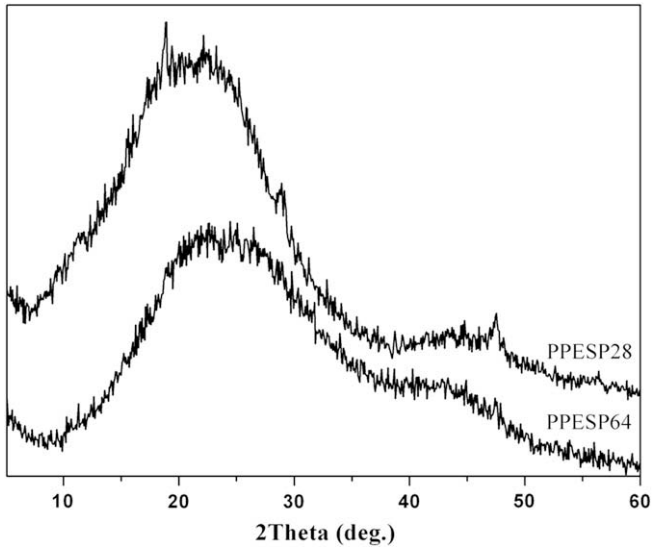

Fig. 9. WAXD diffractograms of PPESP28 and PPESP64.

as the content of sulfone ranges from 20 to 80 mol%, indicating that the presence of sulfone groups hampers the crystallization process. It may be attributed to the highly kinked conformations of copolymer backbone, since sulfone groups have the very different bond angles (around 106°) with aromatic ether (around 121°) groups. The amorphous nature of most copolymers is also reflected in their good solubility in common organic polar solvents, whereas the PPESP28 with highest crystallinity exhibits worse solubility than others. Therefore, it was observed that the presence of kinked sulfone units in each of these copolymers might increase intermolecular freedom and polymer-polar solvent interaction significantly, resulting in the improved solubility in organic polar solvents. The amorphous or micro-crystalline nature of these copolymers could be mainly ascribed to the presence of the crank and twisted non-coplanar phthalazinone moiety that disrupts the planarity and symmetry of copolymer chains.

4. Conclusion

A series of novel copoly(arylene ether sulfone phenyl-s-triazine)s containing phthalazinone moiety in the main chain have been successfully synthesized by a simple one-step solution nucleophilic polycondensation starting from HPPZ, BFPT and DCS. The model reactions of BFPT and DCS with phenol were respectively accomplished under similar conditions, and the conversion of BFPT was determined to be a little higher than that of DCS, indicating the slightly higher reactivity of the former dihalide than the latter towards nucleophilic displacement. High-molecular-weight copolymers were readily achieved in essentially quantitative yields under much milder reaction conditions than those of the known PAEPs. Unlike the known PAEPs, the obtained copolymers demonstrate good solubility in common organic solvents and can be easily cast into transparent flexible films through direct solution casting techniques. The random copolymers show high T_gs and excellent thermal stability. The thermal properties and solubility can be adjusted by varying the content of sulfone units in the polymer backbone. Therefore, incorporation of phthalazinone and sulfone into the PAEP backbone is effective in improving their organic solubility while maintaining good thermal stability. Most of the copolymers demonstrate amorphous nature except that PPESP28 gives a typical pattern of micro-crystalline nature. These attracting properties make the resulting copolymers good candidates for processable and heat-resistant polymeric material.

References

[1] Cassidy PE. Thermally stable polymers: synthesis and properties. New York: Marcel Dekker; 1980.
[2] Anderson DR, John MH. J Polym Sci Polym Chem Ed 1966;4(7):1689–702.
[3] Bengelsdorg IS. J Am Chem Soc 1958;80(6):1442–4.
[4] Haddad I, Hurley S, Marvel CS. J Polym Sci Polym Chem Ed 1973;11(11):2793–811.
[5] Keller TM. J Polym Sci Polym Chem Ed 1987;25(9):2569–76.
[6] Sarwade BD, Wadgaonkar PP, Mahajan SS. Eur Polym J 1988;24(11):1057–61.
[7] Yu GP, Wang JY, Liu C, Lin EC, Jian XG. Polymer 2009;50(7):1700–8.
[8] Matsuo S. J Polym Sci Part A Polym Chem 1994;32(11):2093–8.
[9] Fink R, Frenz C, Thelakkat M, Schmidt HW. Macromolecules 1997;30(26):8177–81.
[10] Fink R, Frenz C, Thelakkat M, Schmidt HW. Macromol Symp 1998;125:151–5.
[11] Cho SY, Chang Y, Kim JS, Lee SC, Kim C. Macromol Chem Phys 2001;202(2):263–9.
[12] Harris FW, Lanier LH, Seymour RB. Structure–solubility relationships in polyimides. New York: Academic Press; 1977. p. 183.
[13] Yoshida S, Hay AS. Macromolecules 1995;28(7):2579–81.
[14] Cheng L, Jian XG, Mao SZ. J Polym Sci Part A Polym Chem 2002;40(20):3489–96.
[15] Yagci H, Ostrowski C, Mathias LJ. J Polym Sci Part A Polym Chem 1999;37(8):1189–97.
[16] Meng YZ, Hlil AR, Hay AS. J Polym Sci Part A Polym Chem 1999;37(12):1781–8.
[17] Liang QZ, Liu PT, Liu C, Jian XG, Hong DY, Li Y. Polymer 2005;46(16):6258–65.
[18] Wang JY, Liao GX, Liu C, Jian XG. J Polym Sci Part A Polym Chem 2004;42(23):6089–97.
[19] Gao YR, Wang JY, Liu C, Jian XG. Chin Chem Lett 2006;17(1):140–2.
[20] Jian XG, Meng YZ, Zheng YH, Hay AS. CN Zl Appl No. 93109180.2; 1993.
[21] Atwood TE, Barr DA, Faasey GG, Newton VJ, Rose AB. Polymer 1977;18(4):354–8.
[22] Johnson RN, Farnham AG, Clendinning RA, Hale WF, Merriam CL. J Polym Sci Polym Chem Ed 1967;5(9):2375–98.
[23] Meng YZ, Hay AS, Jian XG, Tjong SC. J Appl Polym Sci 1998;68(1):137–43.
[24] Fox TG. Bull Am Phys Soc 1956;1(1):123–9.
[25] Fines RE, Bartolomucci JP. In: ASM International Handbook Committee, editor. Engineered materials handbook. Engineering plastics, vol. 2. Metals Park, Ohio: ASM International; 1988.
[26] Meng YZ, Jian XG, Xu Y, Qu MJ. Polym Mater Sci Eng 1994;6:85–8.
[27] Gupta YN, Chakraborty A, Pandey GD, Setua DK. J Appl Polym Sci 2004;92(3):1737–48.